

J. Nano- Electron. Phys.
3 (2011) No1, P.155-161

© 2011 SumDU
(Sumy State University)

PACS numbers: 61.46.Bc, 68.37.Og, 78.30.Ly 78.67.Hc, 81.07.Bc

A STUDY OF THE EVOLUTION OF THE SILICON NANOCRYSTALLITES IN THE AMORPHOUS SILICON CARBIDE UNDER ARGON DILUTION OF THE SOURCE GASES

A. Kole, P. Chaudhuri

Energy Research Unit, Indian Association for the Cultivation of Science,
Jadavpur, Kolkata – 700032
E mail: erak@iacs.res.in

Structural evolution of the hydrogenated amorphous silicon carbide (a-SiC:H) films deposited by rf-PECVD from a mixture of SiH₄ and CH₄ diluted in Ar shows that a smooth transition from amorphous to nanocrystalline phase occurs in the material by increasing the Ar dilution. The optical band gap (E_g) decreases from 1.99 eV to 1.91 eV and the H-content (C_H) decreases from 14.32 at% to 5.29 at% by increasing the dilution from 94 % to 98 %. at 98 % Ar dilution, the material contains irregular shape Si nanocrystallites with sizes over 10 nm. Increasing the Ar dilution further to 98.4 % leads to a reduction of the size of the Si nanocrystals to regular shape Si quantum dots of size about 5 nm. The quantum confinement effect is apparent from the increase in the E_g value to 2.6 eV at 98.4 % Ar dilution. Formation of Si quantum dots may be explained by the etching of the nanocrystallites of Si by the energetic ion bombardment from the plasma.

Keywords: SILICON CARBIDE, RF- PECVD, AR DILUTION, OPTICAL BAND GAP, SI QUANTUM DOTS, QUANTUM CONFINEMENT.

(Received 04 February 2011)

1. INTRODUCTION

Study of the formation of silicon quantum dots (Si q-dots) which are silicon nanocrystallites having sizes of the order of Bohr atomic radius (~5nm) embedded in high band gap amorphous oxides, nitrides or carbides of silicon is highly interesting from the point of view of understanding the basic physics of the interaction of the light quanta with such quantum size matter. Tuning of the band gap in these materials by controlling the size of the Si q-dots have possible technical application in photoluminescent devices and in for third generation solar cells.[1, 2] Most of the works on Si q-dots in a-SiC matrix used hydrogen dilution of the source gases containing Si and C.[3] In this paper we are reporting our studies on the gradual evolution of the nanocrystalline Si into Si quantum dots in a-SiC:H films by the control of the argon dilution of the source gases.

2. EXPERIMENTAL

The a-SiC:H films were deposited by the conventional rf PECVD technique from a mixture of SiH₄, CH₄, and Ar. Total flow of the process gases was maintained at 100 sccm. SiH₄, and CH₄ were flown at 1:1 ratio and the Ar dilution given by $[Ar] \cdot 100 \% / ([Ar] + [SiH_4] + [CH_4])$ was varied from 94 %

to 98.4 %. The preparation conditions of the samples are given in Table 1. The crystalline structure of the nanophase films was investigated using a Seifert XDAL 3000 X-ray diffractometer, operating in the grazing incident geometry (incident angle of 2°). The incident X-ray wave length was 1.5418 \AA (Cu $K\alpha$ line) at 35 kV and 30 mA. The nanostructure of the films was studied by HRTEM (JEOL 2010). The hydrogen and carbon bondings with silicon was studied by FTIR absorption spectroscopy in the frequency range between 400 and 4000 cm^{-1} . The optical absorption and the band gap of the films were measured by UV-vis spectrophotometer (HITACHI U4100).

Table 1 – Preparation conditions of the samples

| Sample No. | SiH ₄ (sccm) | CH ₄ (sccm) | Ar (sccm) | Temp (°C) | Press (Torr) | Power density (mW/cm ²) |
|------------|-------------------------|------------------------|-----------|-----------|--------------|-------------------------------------|
| #QD1 | 3 | 3 | 94 | 200 | 0.2 | 400 |
| #QD2 | 2 | 2 | 96 | 200 | 0.2 | 400 |
| #QD3 | 1.5 | 1.5 | 97 | 200 | 0.2 | 400 |
| #QD4 | 1 | 1 | 98 | 200 | 0.2 | 400 |
| #QD5 | 0.8 | 0.8 | 98.4 | 200 | 0.2 | 400 |

3. RESULTS

3.1 XRD

No diffraction peak related to crystalline silicon is observed up to a dilution level of 96 % (Curves 1 and 2, Fig. 1). But at 97 % dilution of Ar small, broad but clearly resolved diffraction peaks at $2\theta = 28.4^\circ$, 47.3° , and 56.1° appear corresponding to the (111), (220), and (311) crystal planes of silicon respectively (Curve 3, Fig. 1). [4, 5] With further increase of the dilution level to 98 %, the intensities of all three diffraction peaks are increased while the full widths at half maximum (FWHM) of all these diffraction peaks become smaller [Curve 4, Fig. 1]. An additional peak at 69.2° corresponding to (400) plane of Silicon also appears at this dilution level. The peaks however, becomes broad when the Ar dilution level is further increased to 98.4 % (Curve 5, Fig. 1).

3.2 Optical band gap

The optical absorption of the films were measured by UV-Vis spectroscopy to study the optical band gap of the materials. The band gap was obtained from the commonly used Tauc's formula (equation 1),

$$(\alpha h\nu)^{0.5} = B(h\nu - E_g), \quad (1)$$

where α is the optical absorption coefficient, B is the joint optical density of states, and $h\nu$ is the incident photon energy. [6,7] Fig. 2 shows the Tauc's plot for different diluted films to determine the optical band gap E_g which was obtained from the plot of $(\alpha h\nu)^{0.5}$ versus $h\nu$ by extrapolating the linear portion of the curve to intercept the energy axis (at $\alpha = 0$). It is observed that with increasing Ar dilution from 94 % to 98 % there is a continuous decrease of the band gap from 1.99 eV to 1.91 eV. Increasing the dilution further to 98.4% there is a sharp increase in the band gap to 2.6 eV.

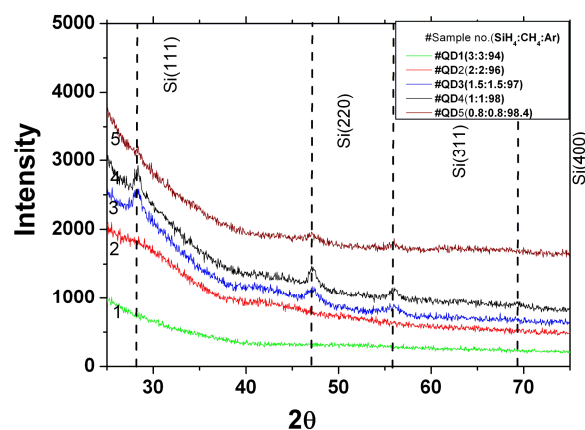


Fig. 1 – XRD pattern of the films deposited under different dilution levels of Ar

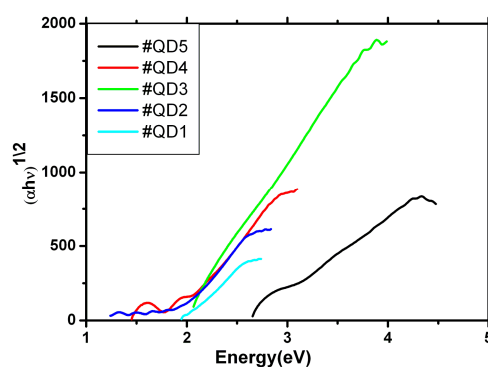


Fig. 2 – Tauc's plot of the a-SiC:H samples deposited at different ar dilution

3.3 FTIR

The nature of the Si-C, Si-H and C-H bonds within the samples deposited at different dilution level of Ar studied by FTIR absorption spectroscopy are shown in Fig. 3. These spectra have been corrected for the substrate absorption and normalized by the film thickness. The main absorption peaks appearing in the spectra are located at (1) $\sim 650\text{cm}^{-1}$, (2) $\sim 780\text{cm}^{-1}$, (3) $\sim 1000\text{cm}^{-1}$, (4) $1900 - 2100\text{cm}^{-1}$ and (5) $2800 - 3100\text{cm}^{-1}$. These peaks are attributed to (1) the wagging or rocking mode of Si-H_n for $n = 1 - 3$, [8], (2) the stretching mode of Si-C, [9], (3) the wagging or rocking mode of C-H_n [10, 11], (4) the stretching mode of Si-H [12] and (5) stretching modes of C-H_n (sp^3) or C-H_n (sp^2) for $n = 1 - 3$ [13] respectively. With the increase in Ar dilution level the intensities of the peaks at $\sim 650\text{cm}^{-1}$ and $\sim 2090\text{cm}^{-1}$ related to Si-H bond decrease. This phenomenon may be associated with the nanocrystalline Si formation in the amorphous matrix. [14] It is also observed that the peak at $\sim 1000\text{cm}^{-1}$ and the absorption band between $2800 - 3100\text{cm}^{-1}$ (both related to C-H_n mode) decrease with the increase in Ar dilution level. This observation together with the decrease

of the Si-C stretching mode at 780 cm^{-1} indicate that the a-SiC:H films are getting Si rich with the increase in Ar dilution level. Hydrogen content (C_H) within the films estimated by de-convoluting the absorbance of Si-H wagging or rocking modes are shown in Fig. 5. It is clear from the graph that with the increasing dilution level the Hydrogen content within the films decreases rapidly which is an important indication of the formation of nano crystallites within the films.

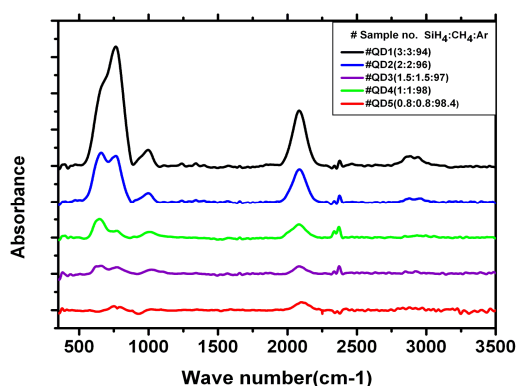


Fig. 3 – FTIR absorption spectra of the films grown at different Ar dilution

3.4 HRTEM

At 94% Ar dilution amorphous nature of a-SiC:H films is apparent from the featureless micrograph (See Fig. 4a). Corresponding SAED (Fig. 4b) shows diffused hallow pattern. With the increase in Ar dilution level diffused rings appear in the SAED indicating formation of the nanocrystallites. The micrograph and the SAED for the 98 % diluted sample are shown in Fig. 4c, d. The micrograph shows randomly oriented nanocrystalline Si of variable sizes. The fringe pattern corresponding to (111) plane of silicon is clearly discernible in the micrograph (Fig. 4c inset). The SAED (Fig. 4d) also shows a sharp ring corresponding to this plane. At 98.4 % Ar dilution the micrograph consists of uniformly distributed nanocrystals of size $\sim 5\text{ nm}$ (Fig. 4e). A distinct feature is observed in the SAED of this film showing a diffused ring with some spots on it. The distinct spots coincide with the Laue spots for the planes (220) and (311) of Si. This unique feature may have appeared in the diffraction pattern when the size of the nanoparticle is reduced to the size of the order of Bohr radius producing the Si quantum dots in the dielectric matrix of SiC.

4. DISCUSSIONS

Formation of Si quantum dots in a host matrix may be achieved along two routes; firstly by the “bottom up” method where the gradual build up of the nanocrystals of the size of “Bohr radius” is achieved by assembling of the Si atoms in a regular arrangement and secondly, by “top down” method where the larger size nanocrystals are etched out to reach the size when the quantum confinement effect will be observed. The XRD data shows a gradual increase of the peaks corresponding to the various planes of

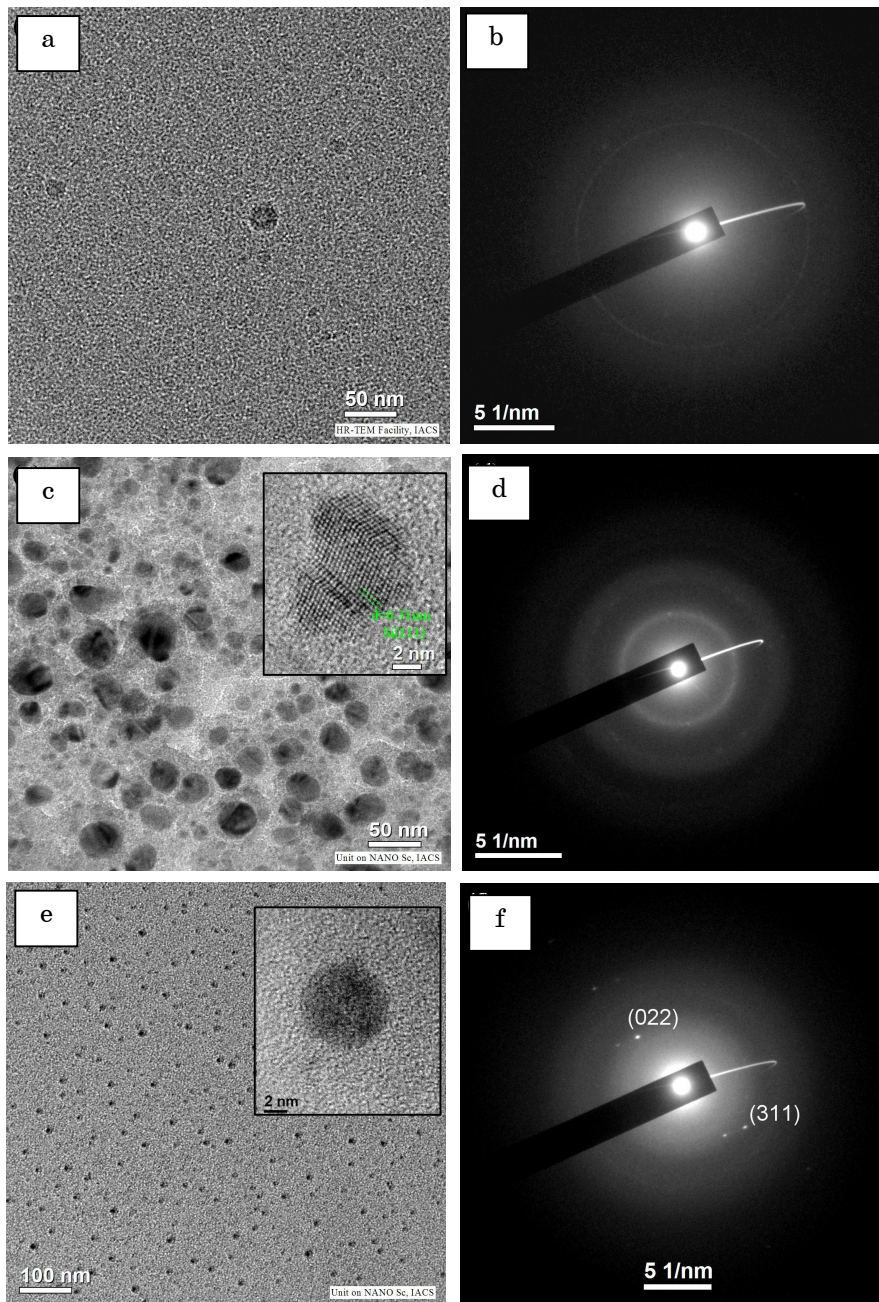


Fig. 4 – HRTEM images of the samples deposited at different Ar dilution. (a), (c), (e) shows the bright field micrograph of the samples deposited at 94 %, 98 % and 98.4 % respectively. (b), (d) and (f) shows the corresponding selected area electron diffraction (SAED) pattern of the samples for 94 %, 98 % and 98.4 % Ar dilution levels respectively

crystalline silicon which indicates increase of the size of the Si nanocrystallites in the a-SiC:H matrix with increase of of Ar dilution from 94 % to 98 %. Increase in the size of the Si nanocrystallites within a-Si has been observed with increasing the dilution of the source gas (SiH_4) with hydrogen has been reported [13]. In this study we observe a broadening of the XRD peaks at the highest dilution level of 98.4 % (Curve 5, Fig. 1). The TEM micrograph of the 98 % Ar diluted sample shows irregular shape large size (> 10 nm) Si nanocrystallites are observed. Corresponding SAED shows rings for Si(111) plane. On increasing the Ar dilution to 98.4 % decrease of the size of the Si nanocrystallites is evident from the inset of the micrograph (Fig. 4e). Corresponding SAED consists of diffused ring with some Laue spots.

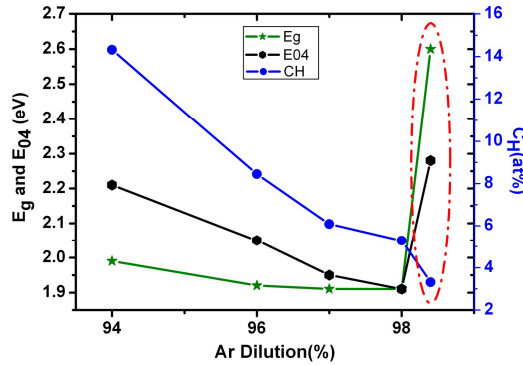


Fig. 5 – Changes in C_H , E_{04} and E_g with Ar dilution

Argon takes leading role in the dissociation of SiH_4 and CH_4 in the plasma as also influencing the surface reactions. While the Ar^+ ions have higher reaction rate with CH_4 , the neutral metastable Ar^* is chiefly responsible for the dissociation of SiH_4 . Thus presence of the relative amounts Ar^* and Ar^+ in the plasma determines the dissociation of SiH_4 and CH_4 . Moreover, bombardment of the growth surface by Ar^+ and Ar^* influences the surface reactions which is important for the evolution of the deposited from amorphous to nanocrystalline phase. Diffused rings containing Laue spots have been observed in the case of Si quantum dots formed within porous silicon [15].

A strong evidence of the Si quantum dot formation in the a-SiC:H matrix is obtained by studying the variation of the E_g and E_{04} with the Ar dilution (Fig. 5). Increase of the size of the Si nanocrystallites causes a decrease of E_g from 1.99 eV to 1.91 eV and E_{04} from 2.21 eV to 1.91 eV by increasing the Ar dilution from 94 % to 98 %. With further increase in the Ar dilution to 98.4% both E_g and E_{04} sharply rises to the values of 2.6 eV and 2.28 eV respectively. Such increase in the band gap can not be explained by the alloying of Si with C or H because both C and H bonding decrease with increasing Ar dilution. Bonded H-content C_H in the material with change in Ar dilution plotted in Fig. 5 show a continuous decrease from 14.32 at% to 3.31 at% with increase in Ar dilution from 94 % to 98.4 %. Reducing the size of the Si crystallites to the size of the Bohr atomic radius (~ 5 nm) has been found to increase the band gap due to quantum confinement effect.

With increasing Ar dilution the growth of amorphous to micro/nano-crystalline silicon occurs through the more and more bombardment of the growth surface by the metastable Ar* atoms and Ar⁺ ions from the plasma. Energy transferred to the surface increases the mobility of the surface adatoms helping in the formation of the nanocrystallites [16]. At higher Ar dilution the momentum transfer to the surface causes etching from the surface. The nanocrystallites are also etched and their size reduced to form silicon quantum dots.

5. CONCLUSION

We have observed that deposition of quantum dots of uniform and regular size in a-SiC:H matrix occurs through the etching out of the initially formed larger size and irregularly shaped nanocrystallites of silicon. Bombardment of the growth surface by the ions from the plasma has been proposed to play a major role in the etching process.

REFERENCES

1. S.M. Kang, S.G. Yoon, S.W. Kim, and D.H. Yoon, *J. Nanosci. Nanotechnol.* **8** 3857 (2008).
2. G. Conibeer, M. Green, R. Corkish, Y. Cho, E.-C. Cho, Chu-W. Jiang, T. Fangsuwanarak, E. Pink, Y. Huang, T. Puzzer, T. Trupke, B. Richards, A. Shalav, K.-L. Lin, *Thin Solid Films* **511**, 654 (2006).
3. Y. Kurokawa, S. Tomita, S. Miyajama, A. Yamada, M. Konagai, *Jap. J. Appl. Phys.* **46** L833 (2007).
4. Q.J. Cheng, S. Xu, S.Y. Huang, K. Ostrikov, *Cryst. Growth Des.* **9** 2863 (2009).
5. Y. Hotta, H. Toyoda, H. Sugai, *Thin Solid Films* **515** 4983 (2007).
6. Q.J. Cheng, S. Xu, K. Ostrikov, *J. Phys. Chem. C* **113** 14759 (2009).
7. Q.J. Cheng, S. Xu, K. Ostrikov, *J. Mater. Chem.* **19** 5134 (2009).
8. M.H. Brodsky, M. Cardona, J.J. Cuomo, *Phys. Rev. B* **16**, 3556 (1977).
9. Y. Catherine and G. Turban, *Thin Solid Films* **60** 193 (1979).
10. H. Wieder, M. Cardona, and C.R. Guarnieri, *phys. status solidi B* **92**, 99 (1979).
11. W. Yu, X. Wang, W. Lu, S. Wang, Y. Biana, G. Fu, *Physica B* **405** 1624 (2010).
12. A. Bhaduri, A. Kole, P. Chaudhuri, *phys. status solidi C* **7**, 774 (2010).
13. Q. Cheng, E. Tam, S. Xu, K. Ostrikov, *Nanoscale* **2**, 594 (2010).
14. A. Chowdhury, S. Ray, *phys. status solidi C* **7**, 628 (2010).
15. Z. Yamani, O. Gurdal, A. Alaql, M.H. Nayfeh, *J. Appl. Phys.* **85**, 8050 (1999).
16. U.K. Das, P. Chaudhuri, S.T. Kshirsagar, *J. Appl. Phys.* **80**, 5389 (1996).